Electronic Supplementary Material (ESI) for Physical Chemistry Chemical Physics.
This journal is © the Owner Societies 2023

Electronic Supporting Information

The Plasmonic Effect of Cu on Tuning CO_2 Reduction Activity and Selectivity

Jing Xue,[ab] Zhenlin Chen,[ab] Kun Dang,[ab] Lei Wu,[ab] Hongwei Ji,[ab] Chuncheng Chen,[ab] Yuchao Zhang*[ab] and Jincai Zhao[ab]

[a] Key Laboratory of Photochemistry, Beijing National Laboratory for Molecular Sciences, Institute of Chemistry, Chinese Academy of Sciences, Beijing 100190, PR China.

[b] University of Chinese Academy of Sciences, Beijing 100049, P. R. China.

* Corresponding author. Email: yczhang@iccas.ac.cn

Experimental details

Chemicals

Copper sulfate pentahydrate ($CuSO_4 \cdot 5H_2O$, ≥99.0%), potassium hydrogen carbonate ($KHCO_3$, ≥99.7%) were purchased from Sigma Aldrich. Sodium hydroxide (NaOH, >99.0%), boric acid (H_3BO_3, >99.5%), phosphoric acid (H_3PO_4, 85%) were purchased from Inched. Anodic aluminum oxide (AAO, DP125-070-50000) template was purchased from Topmembranes Technology Co. Ltd. All the chemicals were used without purification. Deionized water was filtered by equipment (Millipore, Milli-RO Plus) in the laboratory. The Cu foil (99.9%, Alfa Aesar, 2 × 4 cm^2) was sonicated for 30 min in acetone and ethanol for cleaning, and then electropolished in 85% H_3PO_4 at 2.0 V vs. graphite rod for 5 min. The Cu foil was subsequently rinsed with deionized water and blown dry with argon gas (Ar).

Characterization

Scanning electron microscopy (SEM) images were obtained with a Hitachi S4800 scanning electron microscope (Hitachi Ltd.) operated at an acceleration voltage of 10 kV. Transmission electron microscopy (TEM) and High-resolution transmission electron microscopy (HRTEM) images were taken on a JEOL JEM-F200 microscope operating at an accelerating voltage of 200 kV. Ultraviolet-visible (UV-vis) diffuse reflectance spectrum was acquired on a Hitachi U-3900 spectrometer with $BaSO_4$ as the reference. X-ray diffraction (XRD) patterns were obtained on a Bruker D8 Focus X-ray diffractometer with Cu Kα radiation (λ = 1.5405 Å). X-ray photoelectron spectroscopy (XPS) measurements were performed on the Thermo Scientific ESCALab 250Xi using 200 W monochromatic Al Kα radiation, and the spectra were calibrated by C1s peak at 284.8 eV. The transient photovoltage (TPV, CEL-TPV2000, Beijing China Education AU-LIGHT Technology Co., Ltd.) measurements were performed with a 355 nm laser under an open-circuit condition. Raman spectra were collected using a confocal Raman microscope (Horiba LabRAM HR Evolution) with an excitation wavelength of 785 nm and a 50× objective. Each Raman spectrum was acquired over a collection time of 60 s and is the average of two measurements.

Formula derivation

The activation free energy of the reaction exhibits linear relationship with the reaction free energy, leading to the dependence of the reaction rate on the reaction free energy,[1] as shown in equ (S1):

$$RT\ln\left(\frac{rate}{A}\right) = -\Delta G \qquad \text{(S1)}$$

where R is the gas constant (8.314 J mol^{-1} K^{-1}), T is the temperature (K), A is the rate constant, and ΔG is the standard Gibbs free energy (J mol^{-1}). For an electrochemical half-reaction, there is an additional free energy contribution E (the applied potential), and the reaction rate is replaced by the current density (j), therefore the Butler-Volmer relationship can be obtained, as shown in equ (S2):

$$RT\ln\left(\frac{j_{dark}}{A'}\right) = -\Delta G + \theta nFE \qquad \text{(S2)}$$

where j_{dark} is the current density in the dark, A' is the constant with units of the current density, θ is the phenomenological constant that incorporates the charge transfer coefficient, n is the number of electrons involved in the electrochemical reaction, and F is the Faraday constant. Under light irradiation, Cu NAs induced the generation of a photopotential, contributing an additional term of free energy, denoted as G_{photo}. As shown in equ (S3):

$$RT\ln\left(\frac{j_{photo}}{A'}\right) = -\Delta G + \theta nFE + G_{photo} \qquad \text{(S3)}$$

where j_{photo} is the current density under the light. When equ (S2) and equ (S3) are combined, equ (S4) is obtained:

$$RT\ln\left(\frac{j_{photo}}{A'}\right) = RT\ln\left(\frac{j_{dark}}{A'}\right) + G_{photo} \qquad \text{(S4)}$$

It is reported that the free energy contribution of electron-hole pairs generated by LSPR excitation scales linearly with the incident light intensity, I. Therefore, equ (S5) can be obtained:

$$RT\ln\left(\frac{j_{photo}}{A^{'}}\right) = RT\ln\left(\frac{j_{dark}}{A^{'}}\right) + \Phi I \qquad \text{(S5)}$$

where Φ is the photochemical conversion coefficient (s cm^2 mol^{-1}), which represents the free energy contributed to the CO_2RR by LSPR excitation of an incident intensity of 1.0 W cm^{-2}.

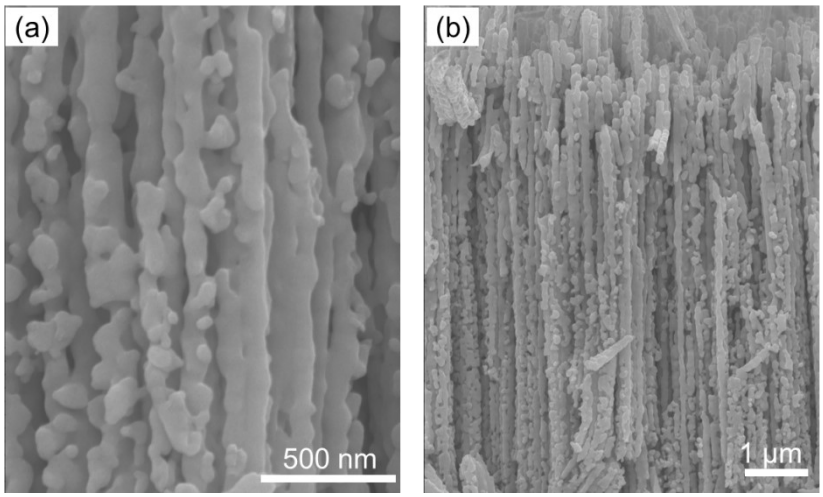

Fig. S1 (a, b) SEM images of Cu NAs after the PEC reduction process.

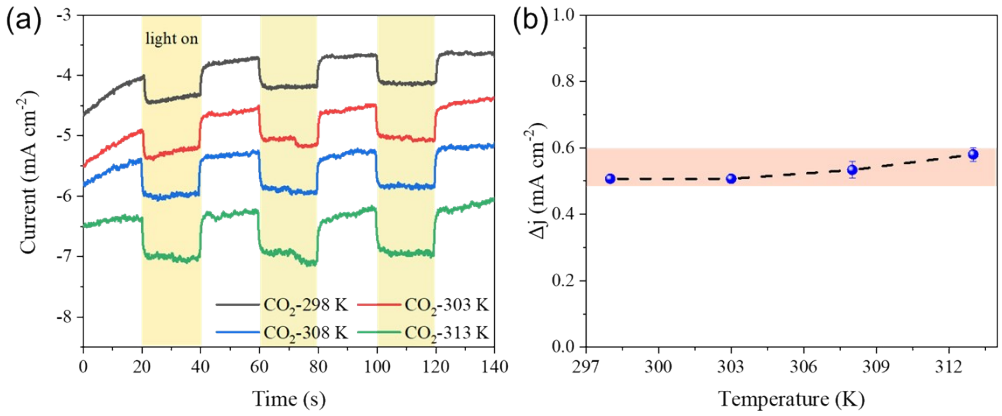

Fig. S2 (a) Chronoamperometry (CA) curves of the Cu NAs photocathode with different temperatures at -0.6 V_{RHE} under chopped light irradiation with an interval of 20 s. (b) The Δj (j_{photo} - j_{dark}) at -0.6 V_{RHE} as the function of the temperature.

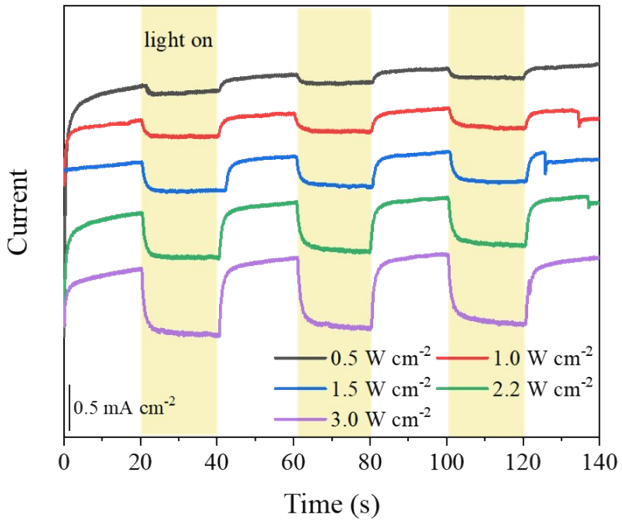

Fig. S3 CA curves of the Cu NAs photocathode with different light intensities at -0.7 V_{RHE} under chopped light irradiation with an interval of 20 s.

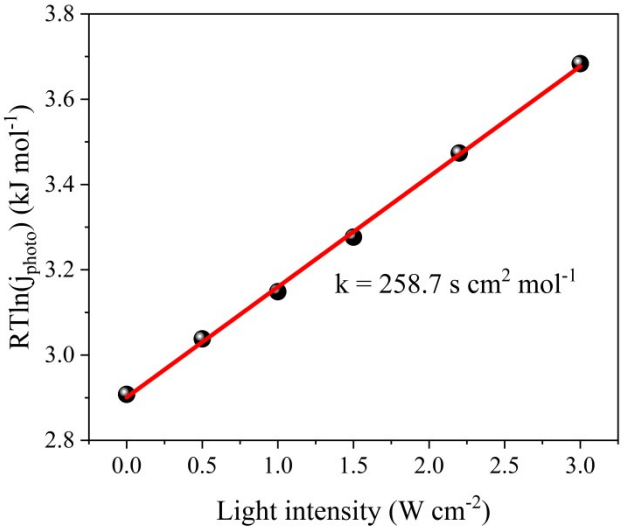

Fig. S4 A plot of RTln(j_{photo}) as a function of the incident light intensity for CO_2RR on the Cu NAs photocathode under visible light irradiation.

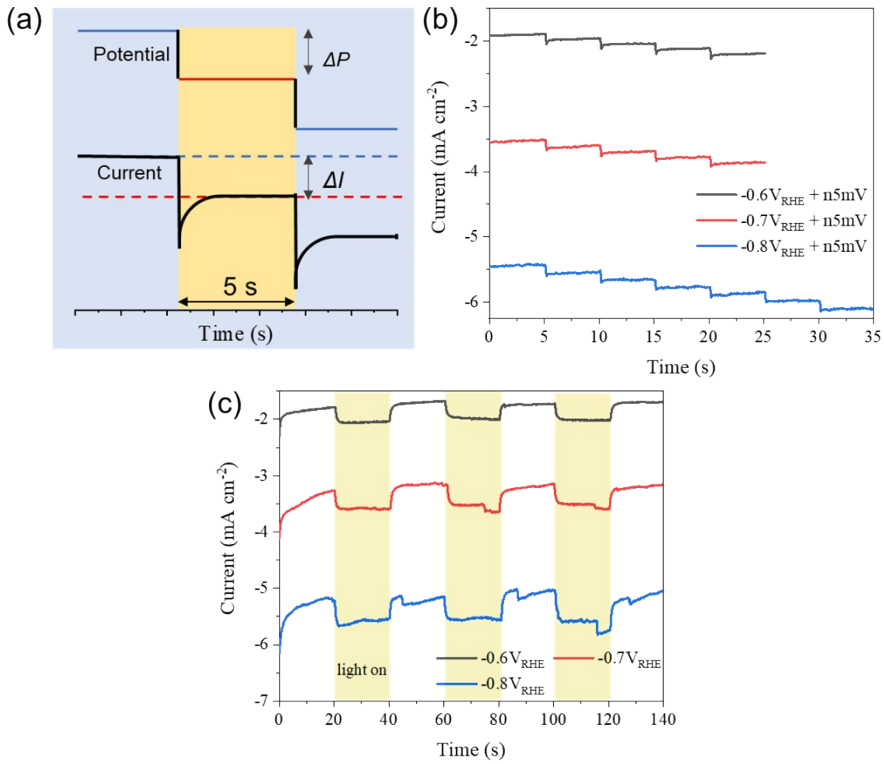

Fig. S5 (a) Schematic of i-t curves in response to a potential step. *ΔI* is the current change induced by the step potential (*ΔP*) after an interval of 5 s to stabilize. (b) The change of current as a function of the step potential (5 mV) at different applied potentials in the dark. (c) CA curves of the Cu NAs photocathode with different applied potentials under chopped light irradiation with an interval of 20 s.

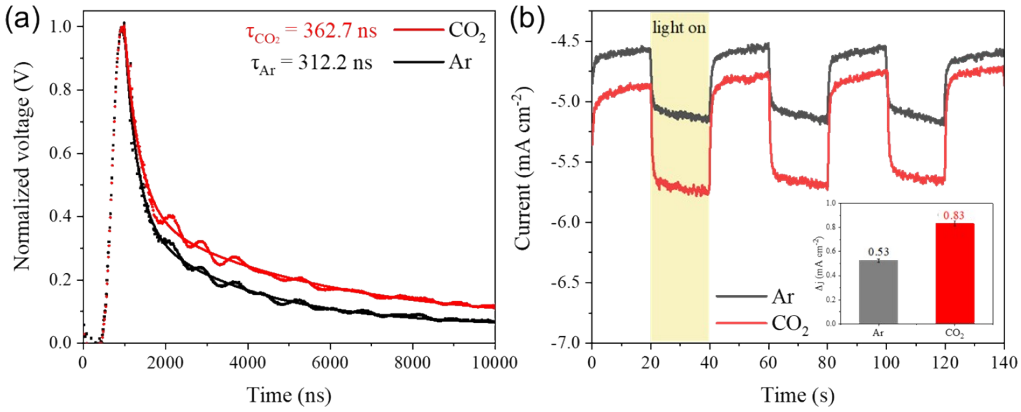

Fig. S6 (a) TPV spectra of the Cu NAs photocathode measured in 0.1 M $KHCO_3$ with Ar (black) or CO_2 (red) atmosphere under open-circuit potential. (b) CA curves of the Cu NAs photocathode with Ar (black) and CO_2 (red) atmospheres at -0.7 V_{RHE} under chopped light irradiation with an interval of 20 s. The insert was Δj at Ar (black) and CO_2 (red) atmospheres.

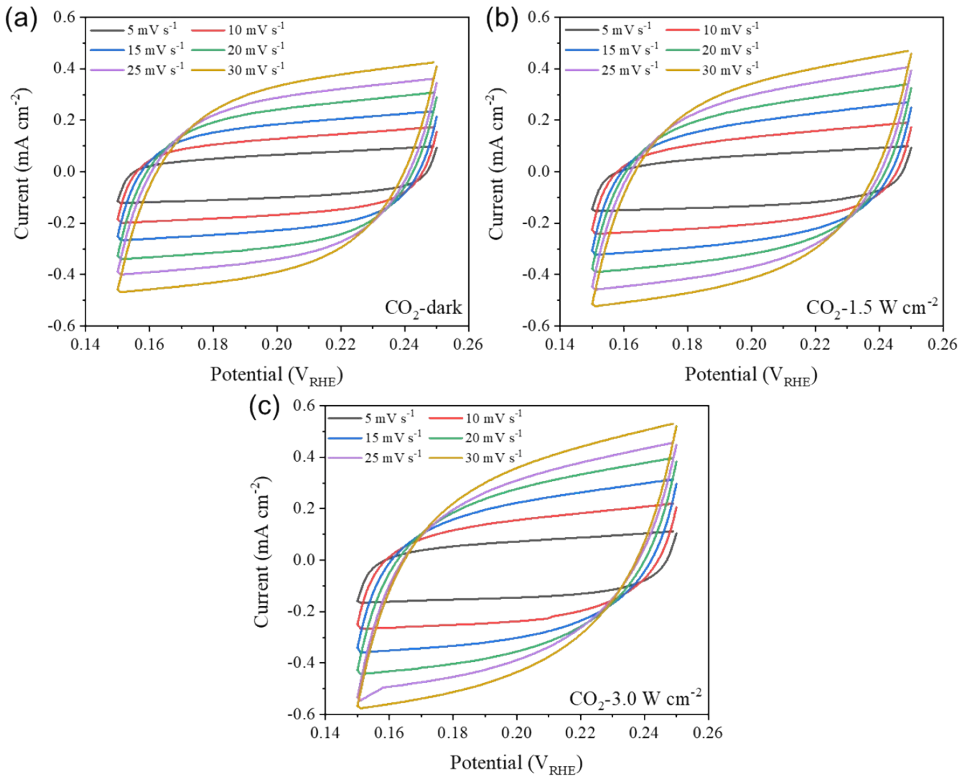

Fig. S7 The CVs measured in aqueous 0.1 M $KHCO_3$ electrolyte between 0.15 V_{RHE} and 0.25 V_{RHE} under different light intensities: (a) dark, (b) 1.5 W cm^{-2}, and (c) 3.0 W cm^{-2}.

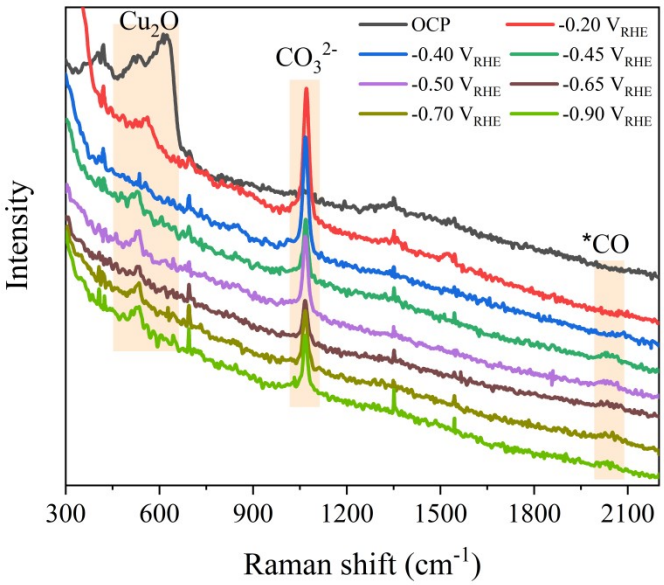

Fig. S8 In situ Raman spectra recorded on Cu NAs during CO_2RR under different applied potentials.

During the CO_2RR process, when the applied cathodic potential increased, Cu_2O was reduced to Cu^0, and Cu_2O (510, 612 cm^{-1}) gradually disappeared.[2] At the same time, CO_3^{2-} were detected, and the intermediate *CO also appeared at -0.45 V_{RHE}.

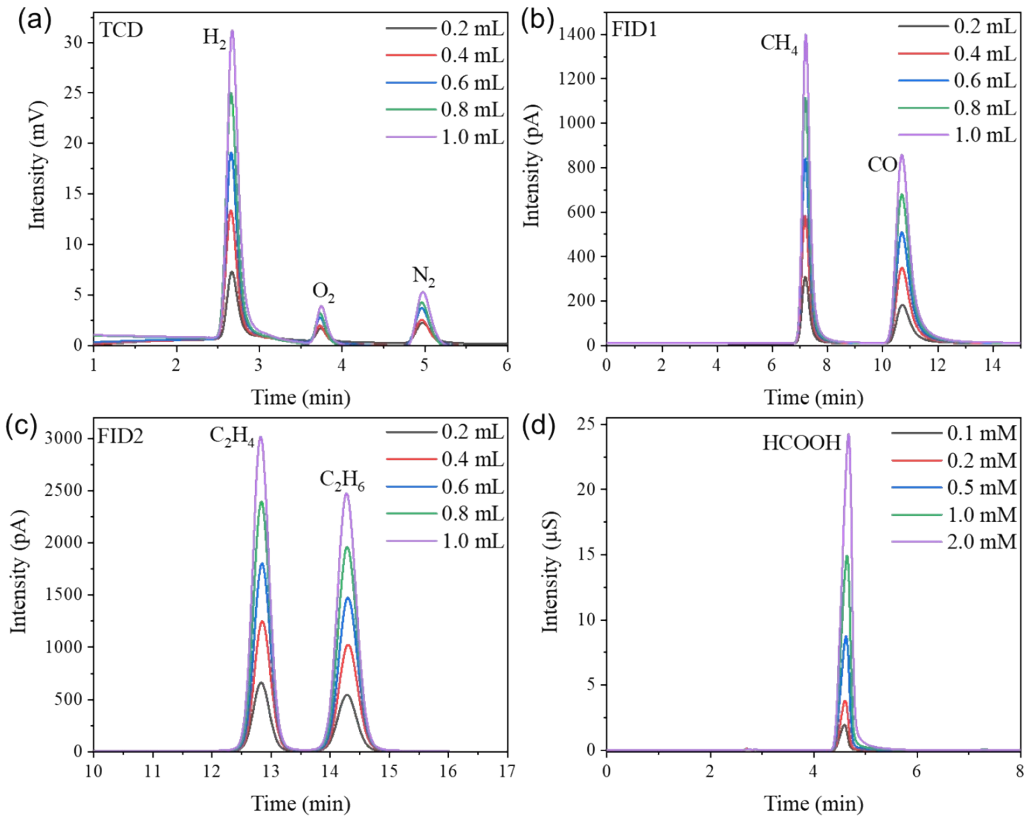

Fig. S9 GC traces of different volumes of standard gases from (a) TCD and (b, c) FID channels. (d) IC signals of HCOOH with different concentrations. Peaks corresponding to the observed gaseous and liquid products are indicated. The gas concentrations are as follows: H_2 (0.502%), CO (0.563%), CH_4 (0.502%), C_2H_4 (0.528%), C_2H_6 (0.506%).

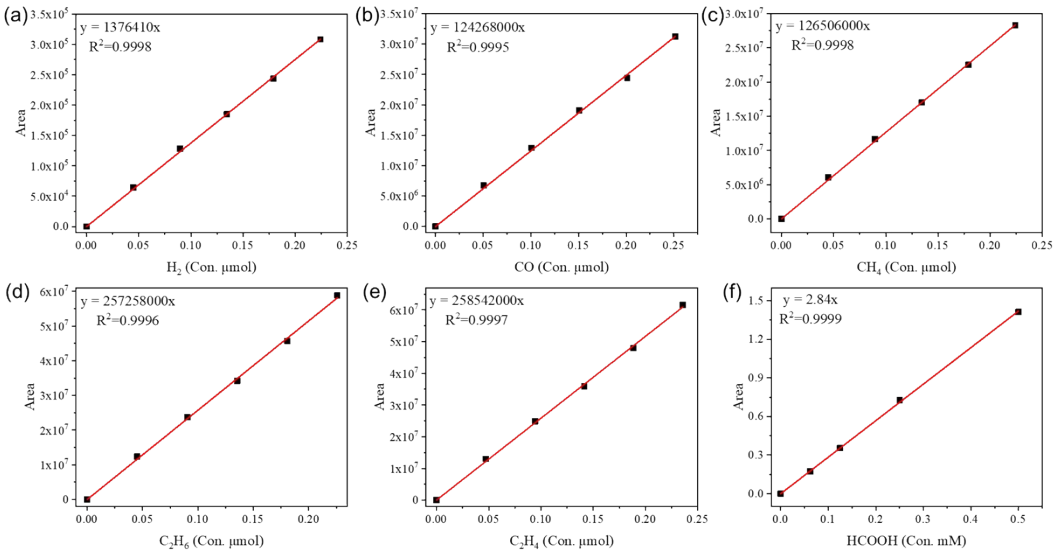

Fig. S10 Standard curves for gas and liquid products.

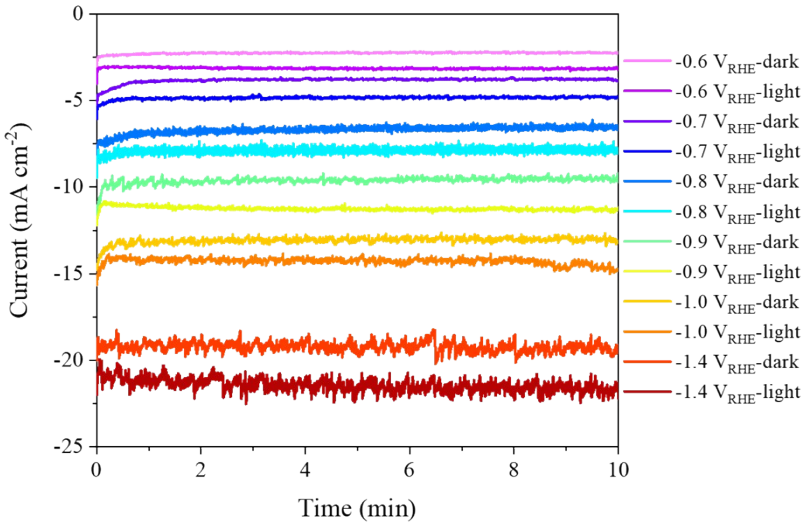

Fig. S11 I-t curves of the Cu NAs photocathode under different potentials in the dark and under light irradiation.

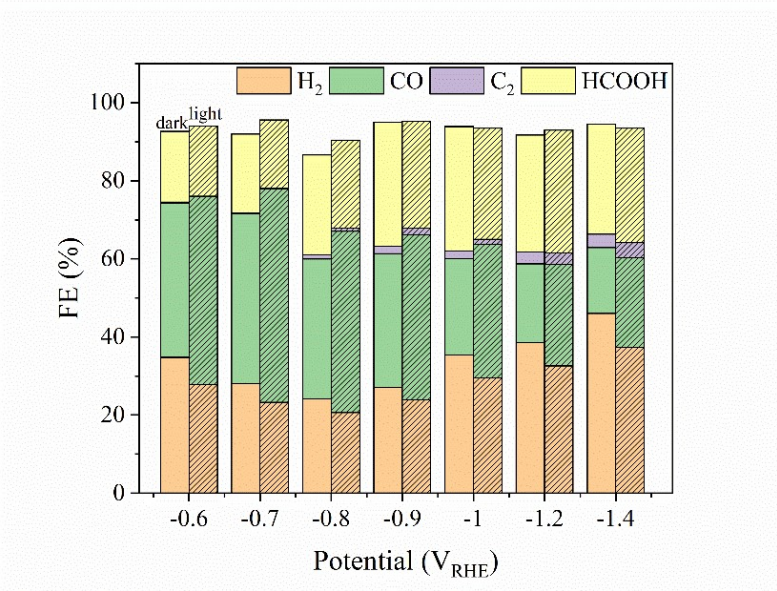

Fig. S12 FE of the gas and liquid products under different applied potentials in the dark and under light irradiation.

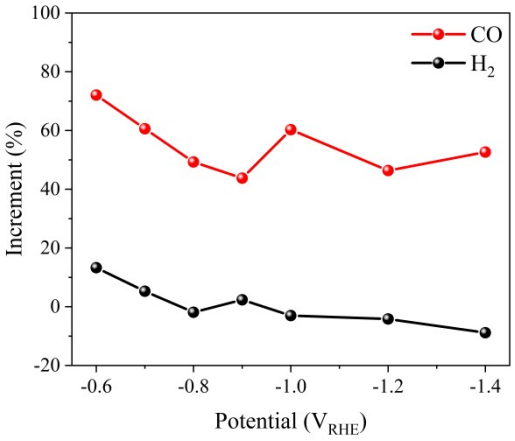

Fig. S13 The increment of H_2 (black) and CO (red) production rates under different applied potentials.

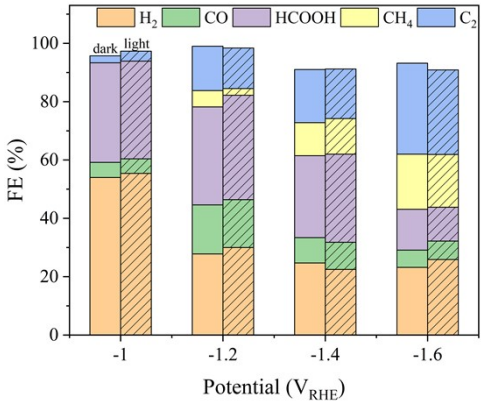

Fig. S14 FE of the gas and liquid products on the Cu foil under different applied potentials in the dark and under light irradiation.

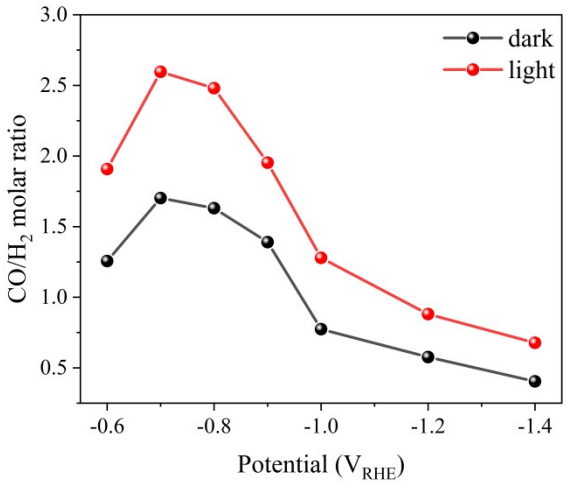

Fig. S15 The molar ratio of CO/H_2 at different potentials in the dark and under light irradiation.

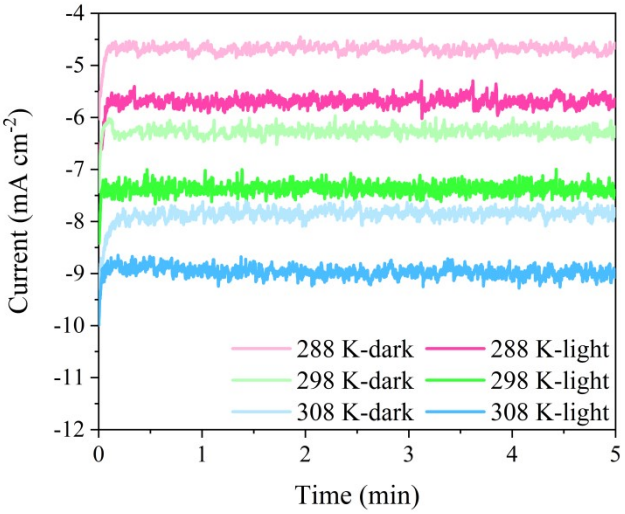

Fig. S16 I-t curves of the Cu NAs photocathode under different temperatures in the dark and under visible light irradiation.

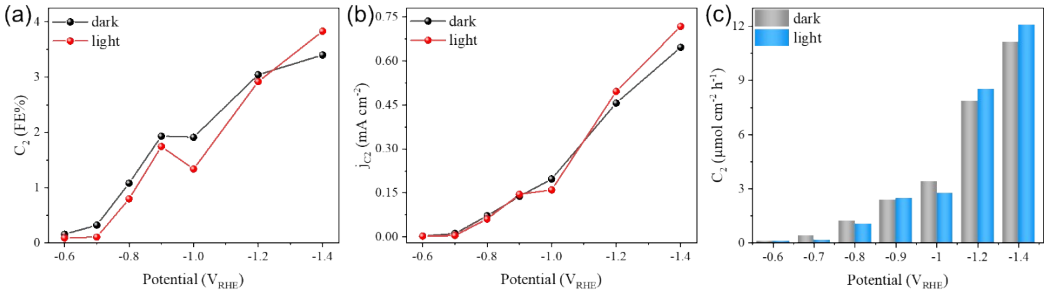

Fig. S17 (a) FE_{C2}, (b) C_2 partial current density (c) and production rate in the dark and under light irradiation under different applied potentials.

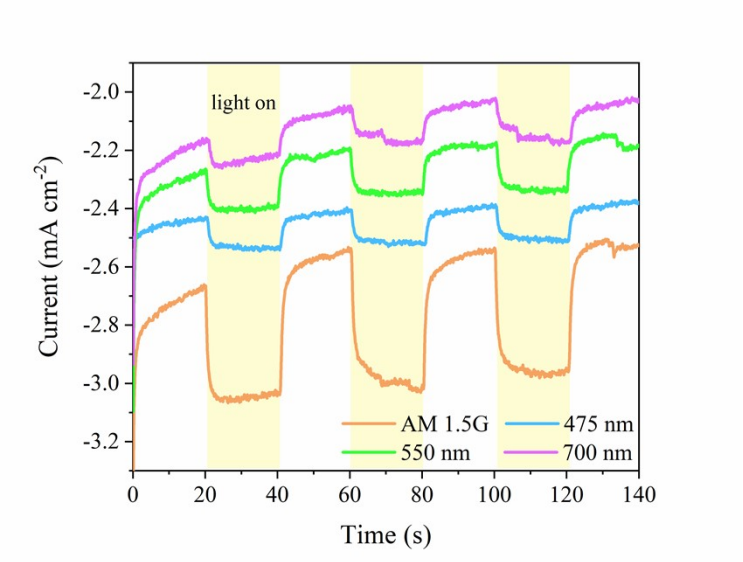

Fig. S18 CA curves of the Cu NAs photocathode with different light sources at -0.7 V_{RHE} under chopped light irradiation with an interval of 20 s.

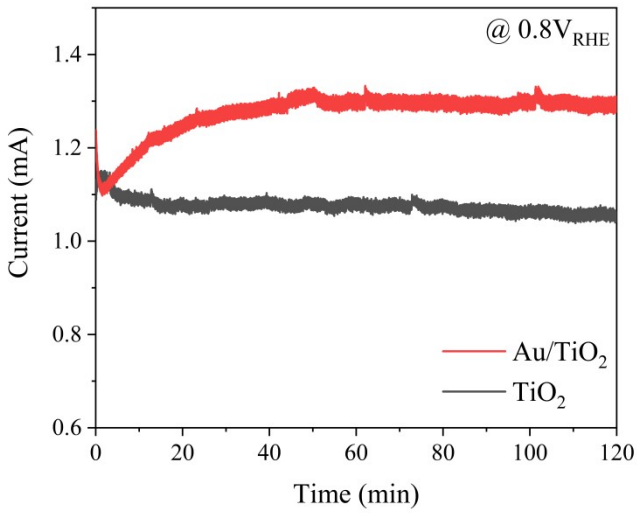

Fig. S19 I-t curves were obtained during the activation of the Au/TiO_2 photoanode at 0.8 V_{RHE} for 2 h under visible light irradiation in 0.5 M potassium borate buffer electrolyte.

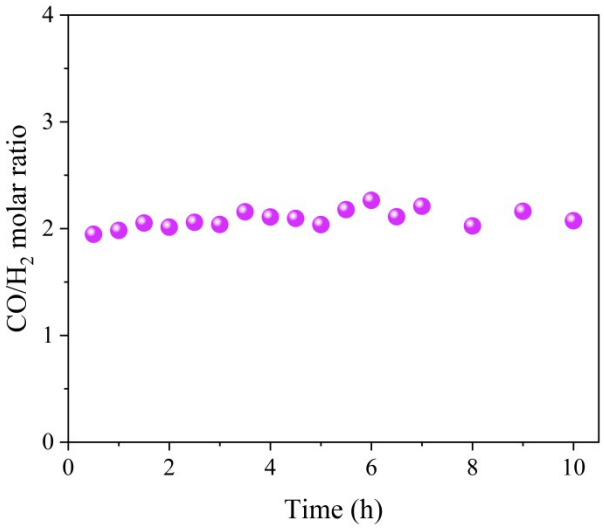

Fig. S20 Stability test of CO/H_2 ratio in the solar-driven PEC device for CO_2RR.

Table S1 The fitted EIS data by using the Cu NAs photocathode under different potentials ranging from -0.5 to -0.8 V_{RHE} in the dark and under light irradiation.

	Potential (V_{RHE})	R_s (Ω)	R_{ct} (Ω)	C_{eff} (mF)
Cu NAs 0.1 M $KHCO_3$ dark	-0.50 V	13.0	123.0	9.77
	-0.55 V	13.3	78.3	9.86
	-0.60 V	13.5	46.5	8.81
	-0.65 V	13.5	32.3	9.17
	-0.70 V	13.6	24.7	11.30
	-0.75 V	13.4	19.8	12.60
	-0.80 V	12.9	17.4	19.20
Cu NAs 0.1 M $KHCO_3$ 3.0 W cm^{-2}	-0.50 V	12.9	78.9	10.40
	-0.55 V	13.2	48.3	10.00
	-0.60 V	13.5	30.8	8.99
	-0.65 V	12.8	21.5	7.18
	-0.70 V	12.8	17.1	8.39
	-0.75 V	13.3	15.2	11.50
	-0.80 V	13.1	13.1	17.60

Table S2 The FE of CO_2RR products by using the Cu NAs photocathode under different potentials ranging from -0.6 to -1.4 V_{RHE} in the dark and under light irradiation.

	Potential (V_{RHE})	Q (C)	H_2 (FE%)	CO (FE%)	HCOOH (FE%)	C_2 (FE%)	FE%
Cu NAs 0.1 M $KHCO_3$ dark	-0.6V – 10 min	0.65	34.76	39.60	18.10	0.16	92.62
	-0.7V – 10 min	1.10	28.10	43.35	20.15	0.32	91.92
	-0.8V – 10min	2.00	24.19	35.75	25.57	1.08	86.59
	-0.9V – 10min	2.15	27.13	34.19	31.72	1.93	94.97
	-1.0V – 10min	3.10	35.31	24.78	31.90	1.91	93.90
	-1.2V – 10min	4.50	38.55	20.15	29.93	3.04	91.67
	-1.4V – 10min	5.70	46.02	16.86	28.12	3.40	94.40
Cu NAs 0.1 M $KHCO_3$ 3.0 W cm^{-2}	-0.6V – 10 min	0.92	27.82	48.13	17.98	0.10	94.03
	-0.7V – 10 min	1.40	23.23	54.70	17.54	0.10	95.57
	-0.8V – 10min	2.30	20.63	46.40	22.54	0.80	90.37
	-0.9V – 10min	2.50	23.88	42.27	27.35	1.75	95.25
	-1.0V – 10min	3.60	29.49	34.20	28.42	1.34	93.45
	-1.2V – 10min	5.10	32.59	26.02	31.42	2.92	92.95
	-1.4V – 10min	6.40	37.35	22.92	29.30	3.83	93.40

Supplemental References

1. J. Wang, J. Heo, C. Chen, A. J. Wilson and P. K. Jain, Ammonia Oxidation Enhanced by Photopotential Generated by Plasmonic Excitation of a Bimetallic Electrocatalyst, *Angew. Chem. Int. Ed.*, 2020, **59**, 18430-18434.
2. Y. Zhao, X.-G. Zhang, N. Bodappa, W.-M. Yang, Q. Liang, P. M. Radjenovica, Y.-H. Wang, Y.-J. Zhang, J.-C. Dong, Z.-Q. Tian and J.-F. Li, Elucidating Electrochemical CO_2 Reduction Reaction Processes on Cu(hkl) Single-Crystal Surfaces by in situ Raman Spectroscopy, *Energ Environ. Sci.*, 2022, **15**, 3968-3977.